

## Combinatorial efficacy of entospletinib and chemotherapy in patient-derived xenograft models of infant acute lymphoblastic leukemia

Joseph P. Loftus,<sup>1\*</sup> Anella Yahiaoui,<sup>2\*</sup> Patrick A Brown,<sup>3</sup> Lisa M. Niswander,<sup>1</sup> Asen Bagashev,<sup>1</sup> Min Wang,<sup>2</sup> Allyson Shauf,<sup>2</sup> Stacey Tannheimer<sup>2</sup> and Sarah K. Tasian<sup>1,4</sup>

<sup>1</sup>Division of Oncology and Center for Childhood Cancer Research, Children's Hospital of Philadelphia, Philadelphia, PA; <sup>2</sup>Gilead Sciences, Foster City, CA; <sup>3</sup>Department of Pediatrics, Division of Pediatric Hematology/Oncology, Johns Hopkins University and Sidney Kimmel Comprehensive Cancer Center, Baltimore, MD and <sup>4</sup>Department of Pediatrics and Abramson Cancer Center, University of Pennsylvania Perelman School of Medicine, Philadelphia, PA, USA

*\*JPL and AY contributed equally as co-first authors.*

©2021 Ferrata Storti Foundation. This is an open-access paper. doi:10.3324/haematol.2019.241729

Received: October 28, 2019.

Accepted: May 8, 2020.

Pre-published: May 15, 2020.

Correspondence: SARAH K. TASIAN - [tasians@chop.edu](mailto:tasians@chop.edu)

---

## SUPPLEMENTAL DATA

### SUPPLEMENTAL METHODS

#### *Cell Titer Glo viability assays*

The human B-acute lymphoblastic leukemia (B-ALL) cell lines NALM-6 (non-*KMT2A*-rearranged) and HB11;19, KOPN-8, and HB11;19 (all *KMT2A*-rearranged) were obtained from the German Collection of Microorganisms and Cell Cultures GmbH (Deutsche Sammlung von Mikroorganismen und Zellkulturen; DSMZ), validated by short tandem repeat identity testing, and confirmed to be *Mycoplasma*-free. ALL cells were incubated *in vitro* with dimethyl sulfoxide or increasing concentrations of entospletinib (Gilead Sciences), fostamatinib (Selleckchem), dasatinib (LC Labs), selumetinib (LC Labs), and/or dexamethasone as indicated in Supplemental Figure 1 for 72 hours, then assessed for cell viability via Cell Titer Glo luminescent assays (Promega) according to manufacturer's instructions using an IVIS Spectrum bioluminescent imaging instrument and Living Image software (PerkinElmer) (1, 2). Data were analysed and displayed graphically in Prism (**Supplemental Figure 1**, **Supplemental Figure 4**, and **Supplemental Figure 5**).

#### *Phosphoflow cytometry*

Viably cryopreserved murine spleen cells from well-engrafted B-ALL PDX models were thawed, washed once in ice-cold serum-free Iscove's modified Dulbecco's medium (IMDM), treated *in vitro* with vehicle, entospletinib, fostamatinib, dasatinib, and/or selumetinib at 37 °C for 60 minutes and then fixed in 16% paraformaldehyde and permeabilized in 90% high-grade methanol as described (3) (**Supplemental Figure 2** and **Supplemental Figure 3**). Human B-ALL cell lines were also incubated *in vitro* with 100 nM, 500 nM, or 1000 nM entospletinib and/or selumetinib in IMDM at 37 °C for 60 minutes prior to fixation and permeabilization as described for phosphoflow cytometry analysis (4, 5) (**Supplemental Figure 6**). Harvested ALL cells from

end-study murine spleens from control or drug-treated PDX models were also analysed by phosphoflow cytometry via the above methodologies (**Figure 6**). ALL cell line and PDX cells were stained with CD45-APC and CD19- APC-eFluor780 (both from EBioscience) cell surface markers and with phosphorylated (p) ERK<sub>T202/Y204</sub>-PacBlue, and pS6<sub>S240/244</sub>-Ax594 or pSYK<sub>Y525/526</sub>-PacBlue (all from Cell Signaling Technologies) intracellular antibodies. Data were collected on a BD FACSVerse flow cytometer with data analysis in Cytobank and graphic display in Prism as described (6).

#### *In vitro colony formation assays*

Viably cryopreserved infant *KMT2A*-rearranged ALL cells harvested from a well-engrafted murine PDX model (ALL3103) were thawed in StemSpan™ SFEM II medium (Stemcell Technologies; Vancouver, BC, Canada) supplemented with recombinant human IL-3 10 ng/mL, granulocyte-macrophage colony-stimulating factor 10 ng/mL, stem cell factor 50 ng/mL (all from Peprotech; Rocky Hill, NJ), and penicillin/streptomycin and rested for 1 hour at 37 °C. ALL cells were subsequently plated in triplicate in 35 mm sterile plates (Cellstar) at 4x10<sup>4</sup> cells/well in cytokine- and antibiotic-containing methylcellulose medium with 25% FBS and 2% BSA and with dimethyl sulfoxide (DMSO; negative control) or increasing concentrations of ENTO. Colony growth was enumerated after 14 days and confirmed to be of lymphoid origin with data analysis and display in Prism (GraphPad; San Diego, CA).

#### *Immunoblotting studies*

Additional ALL PDX cells were thawed and rested for 1 hour at 37°C as above, then treated for 2 hours with 0.1% DMSO or 1 uM entospletinib prior to cell lysis (using Cell Signaling Technology [CST] lysis buffer with protease inhibitor cocktail [Roche Diagnostics] and phosphatase inhibitor sets 1 and 2 [EMD Millipore]) and subsequent evaluation of total and

phosphoprotein expression. Following 30 minutes on ice, cell lysates were cleared by centrifugation at 12,600 rpm for 10 minutes at 4°C. Lysates were analyzed by Simple Western using Peggy Sue™ and Sally Sue™ (ProteinSimple, San Jose, CA; subsequently termed Simple Western).

The following total and phosphorylated protein antibodies were used for Simple Western assays: pERK1/2<sub>T202/Y204</sub>, JAK2, pSTAT5<sub>Y694</sub>, PTEN, pAKT<sub>S473</sub>, pFOXO-1<sub>S256</sub>, pFOXO-1<sub>S319</sub>, FOXO-1, pSRC<sub>Y416</sub>, pLYN<sub>Y396</sub>, ZAP70, pBTK<sub>Y223</sub>, BTK, BCL6, BCL2, BLNK, β-actin (all from CST), p-cMYC<sub>S62</sub>, c-MYC, pFYN<sub>Y530</sub> (Abcam), pBLK<sub>Y389</sub>, pBLK<sub>Y501</sub> (ThermoFisher), pSYK<sub>Y323</sub> (EMD Millipore), and total SYK (Santa Cruz Biotechnology).

#### *In vivo testing of kinase inhibitors and chemotherapy in ALL PDX models*

Following treatment initiation with kinase inhibitors and/or chemotherapy, patient-derived xenograft (PDX) mice were followed by weekly quantitative flow cytometry (FC) analysis of human ALL in retro-orbital venous blood samples and at study endpoint in harvested murine tissues (6). PK analysis of murine blood samples was performed by Gilead Sciences as described (7). Spleen and bone marrow tissues from PD studies were analysed by Simple Western analysis as described below. FC data were captured on a FACSVerse flow cytometer (BD Biosciences) and analysed in Cytobank. Human ALL cell numbers in murine spleens and peripheral blood of vehicle- and drug-treated animals were evaluated for statistical significance by one-way ANOVA with Tukey's post-test for multiple comparisons and displayed graphically in Prism (**Figure 2, Figure 5, Figure 6, Supplemental Figure 7**). Pharmacokinetic-pharmacodynamic correlation analysis was performed in 'short term' AALL3103 PDX mice treated with entospletinib for 72 hours to assess potential dose-dependent inhibition of pSYK<sub>Y323</sub> and pERK<sub>T202/Y204</sub> (**Supplemental Figure 8**).

### *Gene expression analyses*

Gene expression data were analyzed using the NanoStringQCPro R package, version 1.14.10. After positive control normalization and background adjustment using the internal control probes included in the panel, data were log<sub>2</sub>-transformed and normalized using default housekeeping genes. Differential gene expression between *KMT2A-R* versus wild-type or between *KMT2A-MLLT1* versus *KMT2A-AFF1* samples were assessed and compared using the LIMMA R-package (8). Genes with 2-fold difference and p-value <0.05 were identified as significantly expressed (**Supplemental Figure 9**).

### *Immunohistochemistry studies*

Confirmatory immunohistochemical analysis of CD19+ human ALL in harvested murine tissues was performed for some studies. Formalin-fixed, paraffin-embedded ALL-engrafted murine spleen and femur tissues were sectioned (Leica, RM2255 microtome) at 5 µm thickness, placed on Super Frost Plus glass microscope slides (VWR, 48311-703), and baked at 60°C for 20 minutes. Sections were deparaffinized on the DISCOVERY Ultra (Roche Ventana) autostainer at 68°C for 12 minutes. Target epitope retrieval was then performed using heat induced epitope retrieval with Cell Conditioning Solution CC1 (Roche Ventana, 950-124) for 64 minutes at 95°C. The rabbit monoclonal primary anti-CD19 antibody (Abcam, ab134114) was diluted 1:800 in Da Vinci Green diluent (Biocare Medical, PD900M) and incubated for 40 minutes with no heat. A secondary DISCOVERY anti-rabbit-HQ (Roche Ventana, 760-4815) antibody was incubated at 37°C for 32 minutes. The tertiary detection step used DISCOVERY anti-HQ-HRP (Roche Ventana, 760-4820) for 32 minutes at 37°C. Signal visualization used DISCOVERY ChromoMap DAB kit (Roche Ventana, 750-159) at 37°C. Lastly, tissue samples were counterstained with Hematoxylin II (Roche Ventana, 790-2208) at room temperature for 4 minutes.

Upon completion of staining, slides were rinsed in deionized water and soap to remove the oil-based liquid cover slips and were dehydrated by 2 minute incubations in the following

sequence: 1) 70% ethanol 2) 80% ethanol 3) 90% ethanol 4) 100% ethanol 5) 100% ethanol 6) xylene 7) xylene. Slides were then cover-slipped using the Dako Coverslipper (Dako, CR100) with 24mm x 50mm cover glass (Dako, CS70430-2) and mounting media (Dako, CS703) (**Supplemental Figure 10**).

#### *Quantitative Morphometric Measurement of CD19 Staining*

Whole slide-scan images of IHC stained slides were imaged using the Aperio® AT2 (Leica Biosystems) at 40x magnification. Digital slide images were checked for scanning quality, annotated and exported to appropriate network folders within Leica Slidepath Digital Image Hub archive. Quantitative image analysis of CD19-stained tissues was performed on the whole slide-scan images using Visiopharm 2017.2 and the Tissue Find application. A subsequent application was implemented to detect the cells with positive CD19 expression. Positive expression quantification was categorized in three groups (low, medium, high) based on the level of signal intensity and used to calculate an H-score with the equation below (**Supplemental Figure 10**).

$$\%area = \frac{Low\ expression + medium\ expression + high\ expression}{entire\ tissue\ area} \times 100$$
$$H - score = \frac{Low\ expression \times 1 + medium\ expression \times 2 + high\ expression \times 3}{entire\ tissue\ area} \times 100$$

**SUPPLEMENTAL TABLE**

**Supplemental Table 1. Molecular and cytogenetic characteristics of non-infant ALL PDX models.**

<b>ALL PDX model</b>	<b>COG USI</b>	<b>Ph-like</b>	<b>Translocation</b>	<b>Disease status</b>	<b>Other genetic alterations</b>
<b>ALL121</b>	n/a	yes	<i>IGH-CRLF2</i>	relapse	<i>JAK2</i> R683G, <i>CDKN2A/B</i> del
<b>ALL-NT</b>	PATYEI	yes	<i>RCSD1-ABL1</i>	relapse	
<b>PHL3</b>	PANSFD	yes	<i>ETV6-ABL1</i>	<i>de novo</i>	
<b>NH362</b>	PALTWS	no	<i>IGH-CRLF2</i>	<i>de novo</i>	<i>FLT3</i> N609ins23aa
<b>NL432</b>	PAKKCA	yes	<i>EBF1-PDGFRB</i>	<i>de novo</i>	
<b>JL491</b>	PAKMVD	yes	none	<i>de novo</i>	<i>JAK1</i> S646F
n/a	PAXDBJ	yes	<i>GOLGA5-JAK2</i>	<i>de novo</i>	<i>CDKN2A/B</i> del, <i>IKZF1</i> del, <i>PAX5</i> del
n/a	PAVCRK	yes	<i>IGH-EPOR</i>	<i>de novo</i>	<i>CDKN2A/B</i> del, <i>IKZF1</i> del
<b>ALL245</b>	PAWTKG	yes	<i>IGH-CRLF2</i>	<i>de novo</i>	<i>JAK1</i> R629_I631delinsPL, <i>IKZF1</i> del

COG USI = Children's Oncology Group unique specific identifier, del = deletion, mut = mutation, n/a = not available, Ph-like = positive kinase expression signature by low-density microarray testing. Some ALL PDX models were previously published in Maude *et al* Blood 2012, Iacobucci *et al* Cancer Cell 2016, Tasian *et al* Blood 2017, and Ding *et al* Haematologica 2018.

## SUPPLEMENTAL FIGURES

**Supplemental Figure 1. Viability assays of SYK inhibitor-treated *KMT2A*-rearranged ALL cell lines.** Non-*KMT2A*-rearranged (NALM-6) and *KMT2A*-rearranged (HB11;19, KOPN-8, SEM) B-ALL cell lines were treated *in vitro* with kinase inhibitors entospletinib, fostamatinib, or dasatinib at the indicated concentrations for 72 hours, and cell viability was assessed via Cell Titer Glo assays. Half-maximal inhibitory concentrations (IC50) for each inhibitor and cell line are tabulated and displayed. *KMT2A*-rearranged cell lines show similar sensitivity profiles to the more selective SYK inhibitors entospletinib and fostamatinib (with the exception of KOPN-8), but are relatively resistant to the multi-kinase inhibitor dasatinib.

**Supplemental Figure 2. Basal signaling activation in non-*KMT2A*-rearranged and *KMT2A*-rearranged ALL PDX models.** Non-*KMT2A*-rearranged (ALL185GD, ALL83GD, ALL132GD; grey), *KMT2A-AFF1* (ALL150MD, ALL142MD, ALL142MR, ALL3113; dark blue), *KMT2A-MLLT3* (ALL3103MR; red), and *KMT2A-MLLT1* (ALL26MD, ALL26MR, ALL135MD, ALL135MR; light blue) B-ALL PDX cells harvested from viably-cryopreserved murine spleens were thawed and incubated *in vitro* in serum-free medium for 1 hour at 37 °C prior to fixation and permeabilization, cell surface and intracellular antibody staining, and phosphoflow cytometric analysis. Fluorescence-minus-one (FMO) controls were used for each fluorophore-conjugated phosphoprotein antibody to set negative (FMO-) and positive (FMO+) gates. Basal levels of phosphorylated (p) SYK<sub>Y525/526</sub>, pERK1/2<sub>T202/Y204</sub>, and pS6<sub>S240/244</sub> were quantified by phosphoflow cytometry and displayed as percentages of CD45+ CD19+ human ALL cells in FMO+ gates as previously described (6). ALL3113 (dotted dark blue) was created from an adult *KMT2A*-rearranged specimen. All other PDX models were established from *de novo* or relapsed infant ALL specimens from the Children's Oncology Group AALL0631 phase 3 clinical trial or institutional leukemia biorepositories.

**Supplemental Figure 3. Phosphoflow cytometry analysis of kinase inhibitor-treated ALL PDX cells.** Non-*KMT2A*-rearranged (ALL185GD, ALL83GD, ALL132GD) and *KMT2A*-rearranged (all others) B-ALL PDX cells were harvested from murine spleens and treated *in vitro* with 1  $\mu$ M entospletinib, fostamatinib, or dasatinib in serum-free medium for 1 hour at 37 °C prior to fixation and permeabilization, cell surface and intracellular antibody staining, and phosphoflow cytometric analysis as in Supplemental Figure 2. The phosphatase inhibitor pervanadate at 125  $\mu$ M final concentration was used as a positive signaling control (not shown). Phosphoprotein levels were normalized to basal conditions (DMSO-treated controls) in each model, and percent signaling inhibition was calculated for each drug treatment as described (6). Most PDX models demonstrated inhibition of pSYK<sub>Y525/526</sub>, pERK1/2<sub>T202/Y204</sub>, and/or pS6<sub>S240/244</sub> with *in vitro* kinase inhibitor treatment. Similar effects of the selective SYK inhibitors entospletinib and fostamatinib were observed in most models.

**Supplemental Figure 4. *In vitro* and *in vivo* evaluation of entospletinib and dexamethasone in ALL PDX models.** (A) Non-*KMT2A*-rearranged (NALM-6) and *KMT2A*-rearranged (HB11;19, KOPN-8, SEM) B-ALL cell lines were treated *in vitro* with dexamethasone without (left panel) or with 1  $\mu$ M entospletinib (right panel) at the indicated concentrations for 72 hours, and cell viability was assessed via Cell Titer Glo assays. KOPN-8 cells were relatively more glucocorticoid-resistant, but appeared to be resensitized to dexamethasone with concomitant entospletinib exposure. (B) *KMT2A*-rearranged ALL3113MR and (C) non-*KMT2A*-rearranged ALL83GD PDX models were treated with control chow (vehicle [veh]), entospletinib (ento) 0.05% chow continuously provided, dexamethasone (dex) 1 mg/kg intraperitoneally 5 days/week, or both ento and dex for 4 weeks. Human CD45<sup>+</sup> CD19<sup>+</sup> ALL flow cytometric analysis of murine blood at weekly time points (left panels) and spleens at study endpoint (right panels) demonstrated significant inhibition of ALL proliferation with dex treatment (mean  $\pm$  SEM). No additional reduction of splenic leukemia burden was observed in either PDX model with combination ento/dex

treatment. Data were analysed in Prism via ANOVA with Dunnett's (blood data) or Tukey's (spleen data) post-test for multiple comparisons. ns = not significant, \*  $p < 0.05$ , \*\*  $p < 0.01$ , \*\*\*  $p < 0.001$ , \*\*\*\*  $p < 0.0001$ .

**Supplemental Figure 5. Viability assays of kinase inhibitor-treated *KMT2A*-rearranged ALL cell lines.** Non-*KMT2A*-rearranged (NALM-6) and *KMT2A*-rearranged (HB11;19, KOPN-8, SEM) B-ALL cell lines were treated *in vitro* with (A) the SYK inhibitor entospletinib, (B) the MEK inhibitor selumetinib, or (C) and (D) both inhibitors at the indicated concentrations for 72 hours, and cell viability was assessed via Cell Titer Glo assays. RAS-mutant cell lines NALM-6 and KOPN-8 were particularly sensitive to selumetinib.

**Supplemental Figure 6. Phosphoflow cytometry analysis of kinase inhibitor-treated *KMT2A*-rearranged ALL cell lines.** Non-*KMT2A*-rearranged (NALM-6) and *KMT2A*-rearranged (HB11;19, KOPN-8, SEM) B-ALL cell lines were treated *in vitro* with the SYK inhibitor entospletinib and/or the MEK inhibitor selumetinib at the indicated concentrations in serum-free medium for 1 hour prior to fixation and permeabilization, cell surface and intracellular antibody staining, and phosphoflow cytometric analysis as in Supplemental Figure 2. Pervanadate 125  $\mu\text{M}$  final concentration was used as a positive signaling control (not shown).

**Supplemental Figure 7. *In vivo* activity of entospletinib monotherapy in Ph-like ALL.** NH011 PDX mice were treated with vehicle (veh) or ento chow at the specified concentrations (0.03%, 0.07%) for 3 weeks with the same methods used for the ALL3103 model data shown in Figure 2. Human CD45<sup>+</sup> CD19<sup>+</sup> ALL flow cytometric analysis of murine blood at weekly time points (left panel) and spleens at study endpoint (right panel) demonstrated significant inhibition of ALL proliferation with ENTO treatment (mean  $\pm$  SEM). No difference in ALL burden was observed in 0.03% versus 0.07% ENTO-treated animals. Data were analysed in Prism via ANOVA with

Tukey's post-test for multiple comparisons. ns = not significant, \*  $p < 0.05$ , \*\*  $p < 0.01$ , \*\*\*  $p < 0.001$ , \*\*\*\*  $p < 0.0001$ .

**Supplemental Figure 8. Pharmacokinetic and pharmacodynamic correlation in an entospletinib-treated ALL PDX model.** Individual mice from the ALL3103 (*KMT2A-MLLT3*) PDX model treated with ENTO for 72 hours demonstrated a correlation between higher ENTO concentration and lower pSYK Y323 expression (Pearson correlation coefficient  $r = -0.627$ ;  $p = 0.01$ ) and pERK 1/2 expression (Pearson correlation coefficient  $r = -0.303$ ;  $p = 0.31$ ). Terminal spleens were harvested, viably cryopreserved, lysed, and evaluated for levels of pSYK, pERK and  $\beta$ -actin by Simple Western; area under the curve (AUC) values were normalized to  $\beta$ -actin loading control. Terminal blood was collected and evaluated for entospletinib levels.

**Supplemental Figure 9. Immunohistochemical analysis of murine tissues after *in vivo* entospletinib treatment.** CD19 staining via immunohistochemistry (IHC) was performed in harvested spleens and bone marrow of mice engrafted with ALL3103 (*KMT2A-MLLT3*) cells and treated for 4 weeks with vehicle control (saline), 0.07% ENTO chow, 0.25 mg/kg vincristine (VCR), or ENTO and VCR in combination. Percentage represents median of %CD19+ area stained per treatment group. CD19 staining in naïve (non-leukemia-engrafted) mice is displayed in the graph, but not included in statistical analysis. Data are represented as median with interquartile range. \* $p < 0.05$ , \*\* $p < 0.01$ , \*\*\*\*  $p < 0.0001$  by one-way ANOVA with post-hoc Tukey's test for multiple comparisons.

**Supplemental Figure 10. Differential gene expression between *KMT2A*-R and non-*KMT2A*-R PDX models.** Transcriptomic differences between 3 non-*KMT2A*-rearranged (ALL83GD, ALL132GD, ALL185GD) and 8 *KMT2A*-rearranged (others) ALL PDX model samples were evaluated using NanoString. **(A)** Forty-seven upregulated genes and 23 downregulated genes

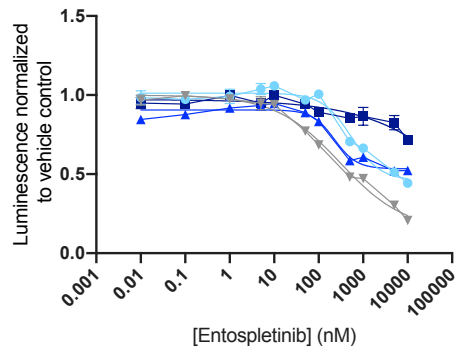
were identified in *KMT2A*-R (left) samples in comparison to non-*KMT2A*-R (right) ALL samples, demonstrating clear separation of these genetic subtypes. **(B)** Further analysis of *KMT2A*-R ALL samples demonstrated 116 significantly differential expressed genes in samples with *KMT2A*-*MLL1* (n=2) versus *KMT2A*-*AFF1* (n=2) rearrangements, including genes involved in DNA repair, cell cycle/apoptosis, and MAPK, PI3K, and RAS signaling pathways.

## SUPPLEMENTAL REFERENCES

1. Gill S, Tasian SK, Ruella M, et al. Preclinical Targeting of Human Acute Myeloid Leukemia and Myeloablation Using Chimeric Antigen Receptor-Modified T Cells. *Blood*. 2014;123(15):2343-2354.
2. Tasian SK, Kenderian SS, Shen F, et al. Optimized Depletion of Chimeric Antigen Receptor T Cells in Murine Xenograft Models of Human Acute Myeloid Leukemia. *Blood*. 2017;129(17):2395-2407.
3. Maude SL, Tasian SK, Vincent T, et al. Targeting Jak1/2 and Mtor in Murine Xenograft Models of Ph-Like Acute Lymphoblastic Leukemia. *Blood*. 2012;120(17):3510-3518.
4. Tasian SK, Doral MY, Borowitz MJ, et al. Aberrant Stat5 and Pi3k/Mtor Pathway Signaling Occurs in Human Crlf2-Rearranged B-Precursor Acute Lymphoblastic Leukemia. *Blood*. 2012;120(4):833-842.
5. Tasian SK, Hurtz C, Wertheim GB, et al. High Incidence of Philadelphia Chromosome-Like Acute Lymphoblastic Leukemia in Older Adults with B-All. *Leukemia*. 2017;31(4):981-984.
6. Tasian SK, Teachey DT, Li Y, et al. Potent Efficacy of Combined Pi3k/Mtor and Jak or Abl Inhibition in Murine Xenograft Models of Ph-Like Acute Lymphoblastic Leukemia. *Blood*. 2017;129(2):177-187.
7. Sharman J, Hawkins M, Kolibaba K, et al. An Open-Label Phase 2 Trial of Entospletinib (Gs-9973), a Selective Spleen Tyrosine Kinase Inhibitor, in Chronic Lymphocytic Leukemia. *Blood*. 2015;125(15):2336-2343.
8. Ritchie ME, Phipson B, Wu D, et al. Limma Powers Differential Expression Analyses for Rna-Sequencing and Microarray Studies. *Nucleic Acids Res*. 2015;43(7):e47.

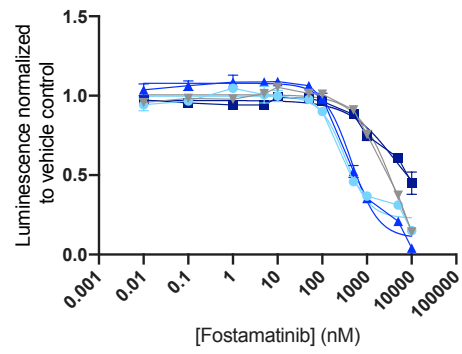
# Supplemental Figure 1

**A**



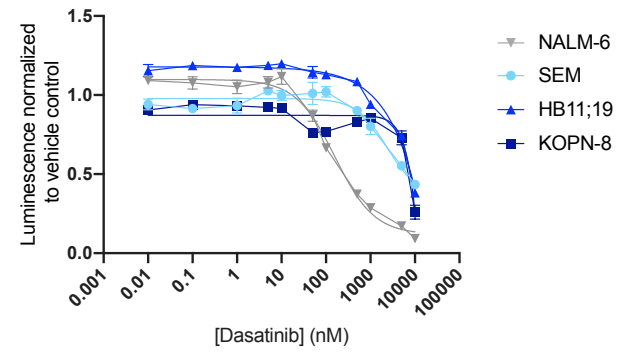
	NALM-6	SEM	HB11;19	KOPN-8
IC50	303.1	542.4	226.4	~ 1904755

**B**



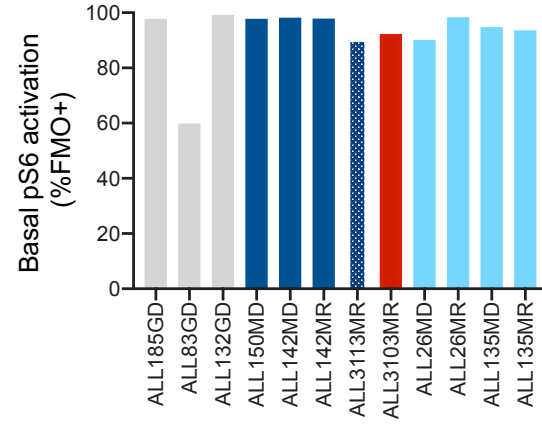
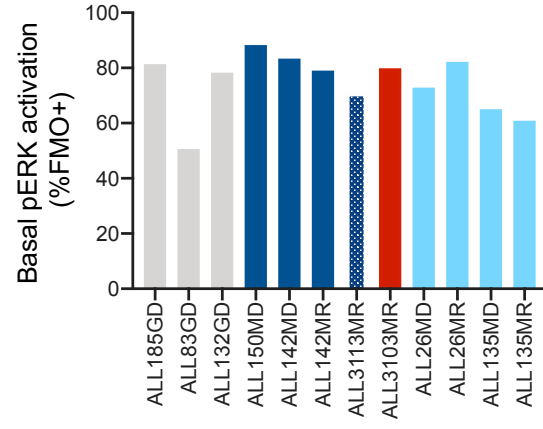
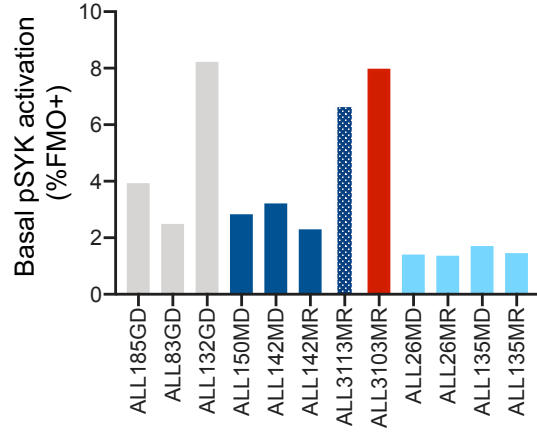
	NALM-6	SEM	HB11;19	KOPN-8
IC50	4312	323.4	445.8	4039

**C**

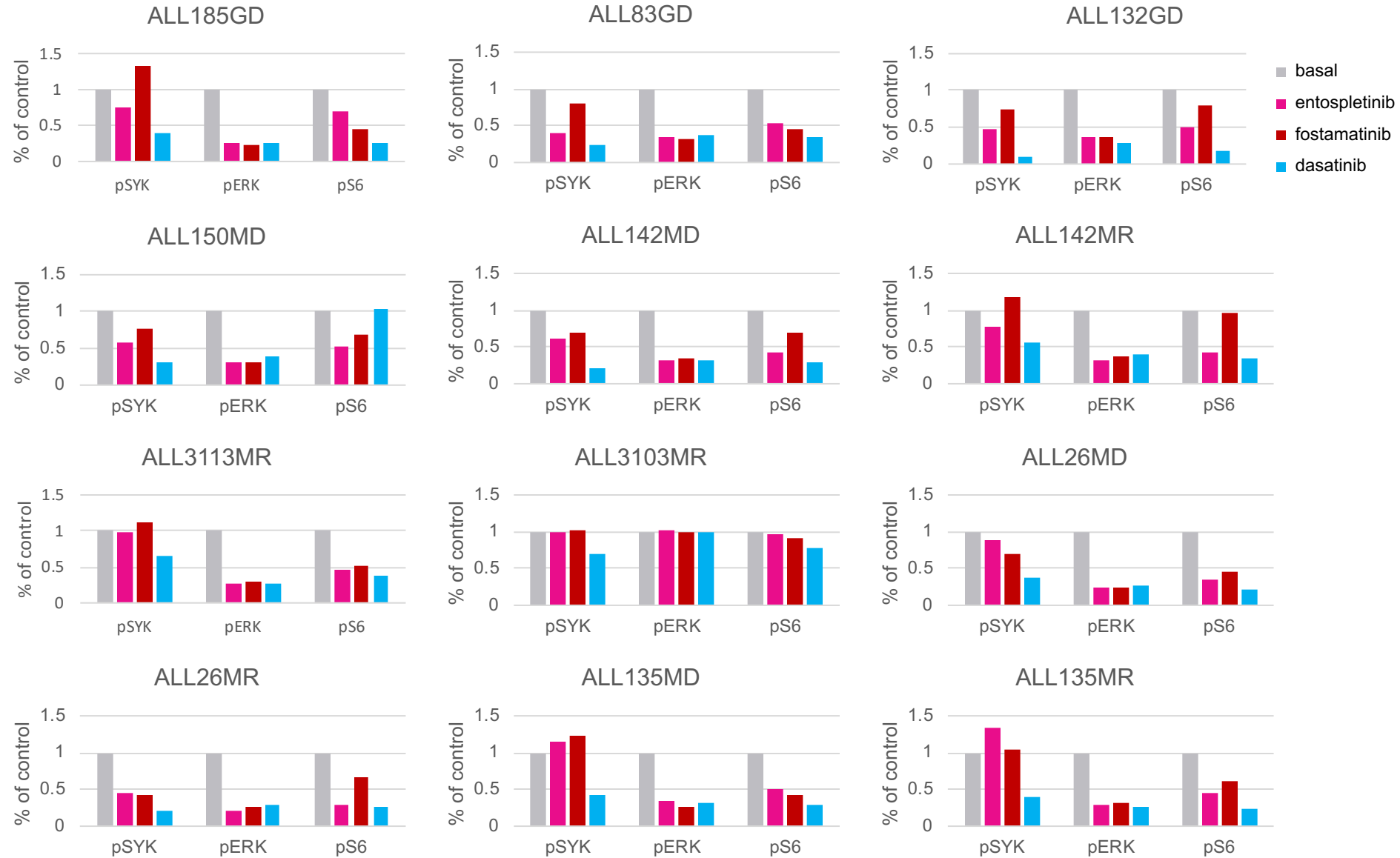


	NALM-6	SEM	HB11;19	KOPN-8
IC50	159.7	2364	~ 18512275	~ 38999

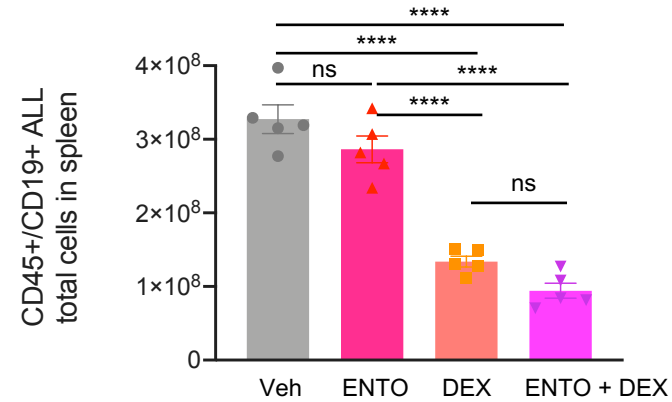
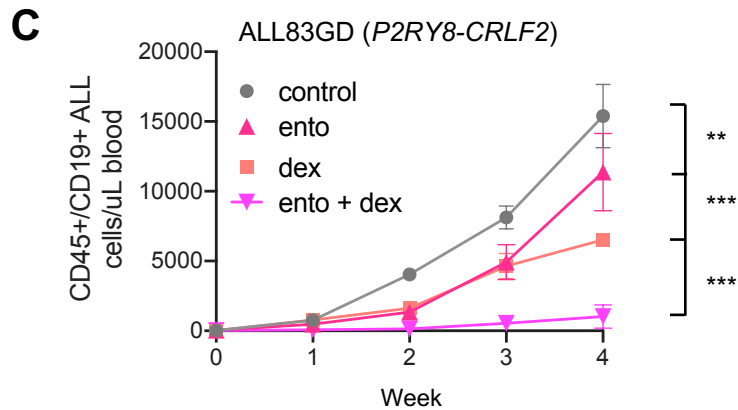
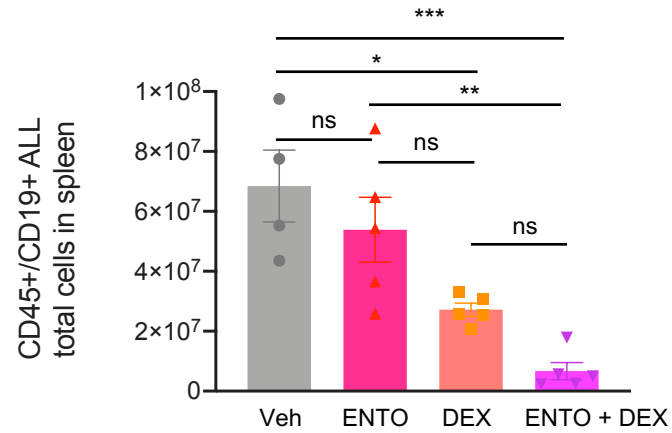
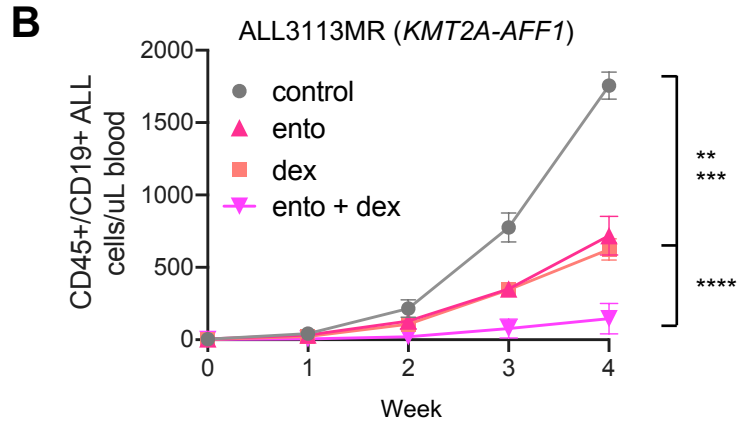
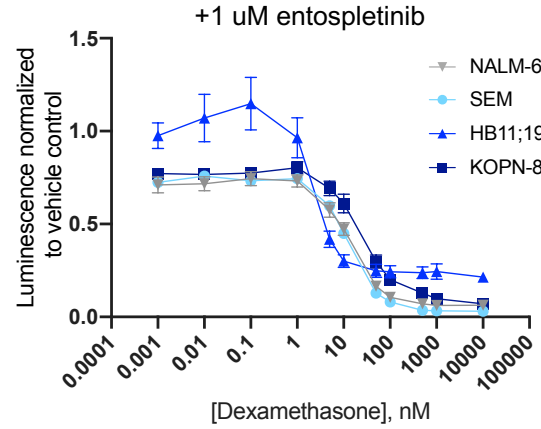
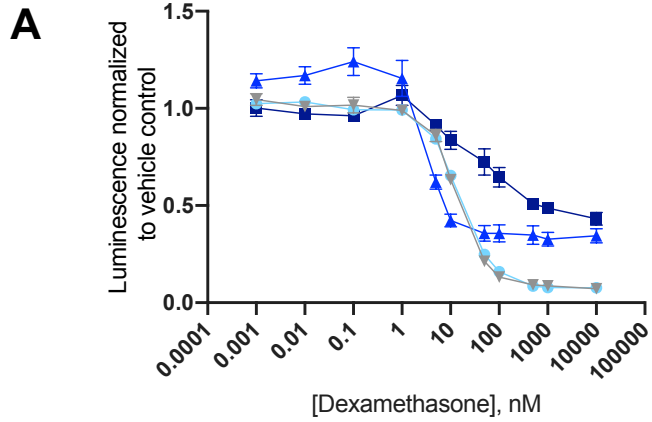
# Supplemental Figure 2



# Supplemental Figure 3

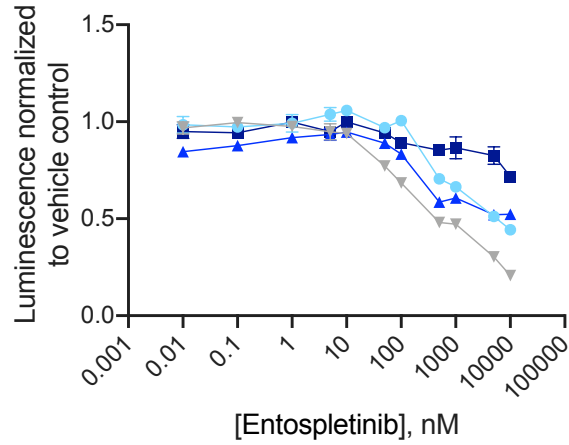


# Supplemental Figure 4

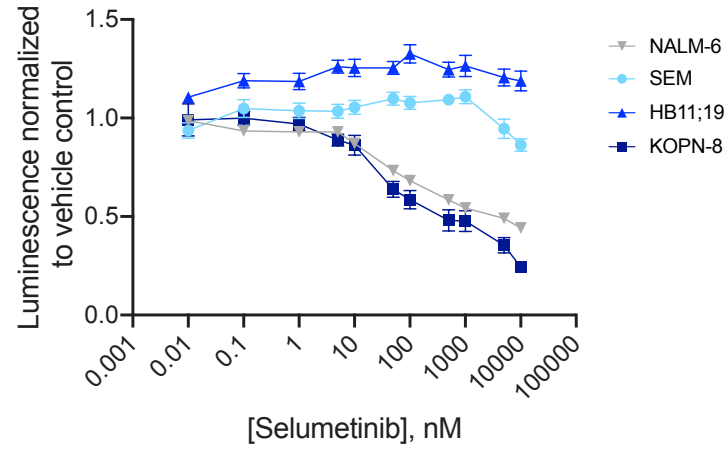


# Supplemental Figure 5

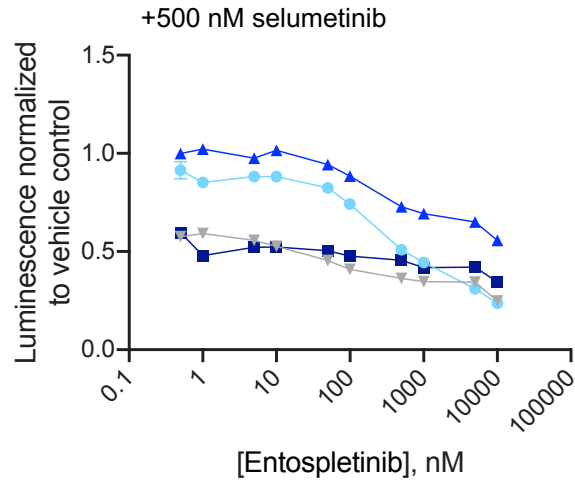
**A**



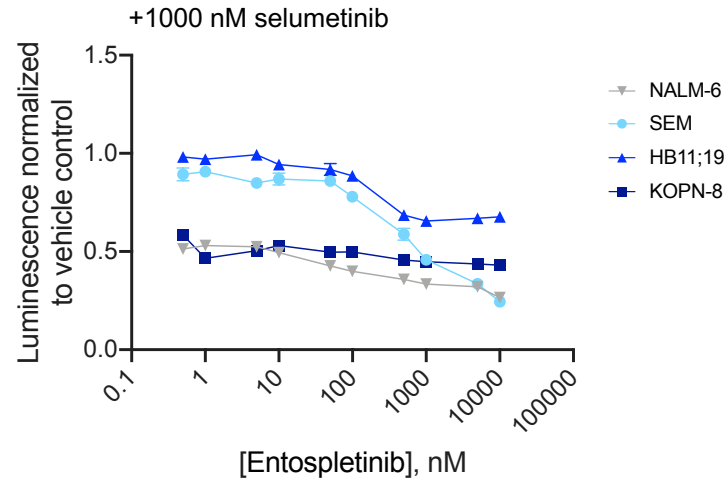
**B**



**C**

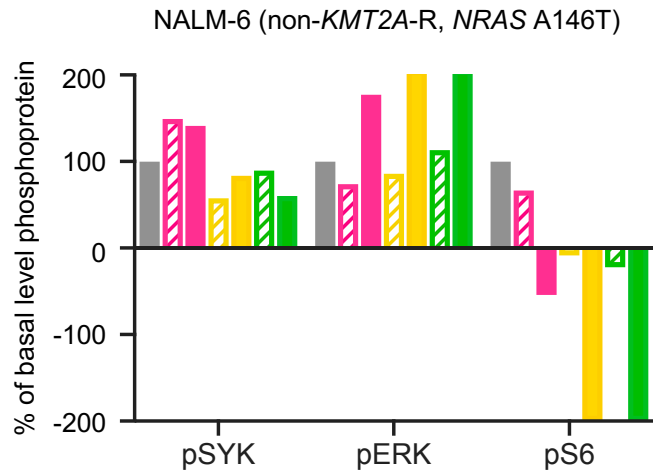


**D**

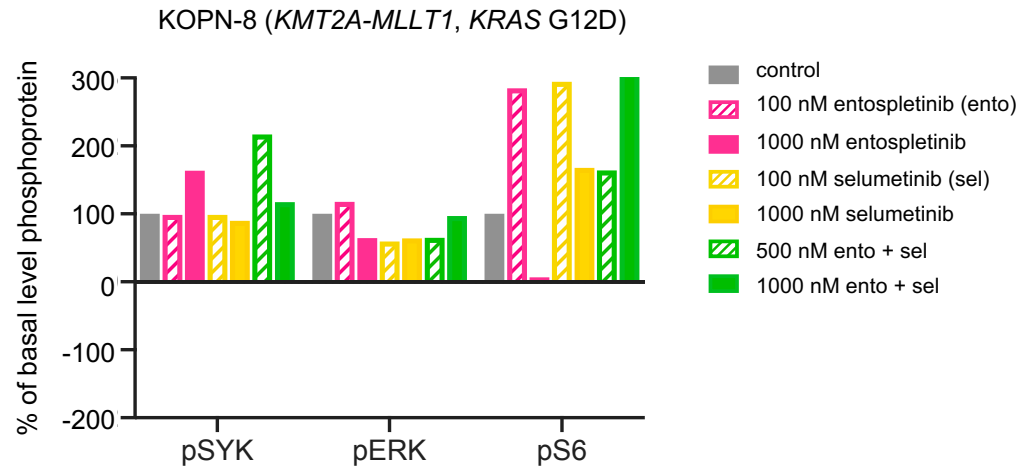


# Supplemental Figure 6

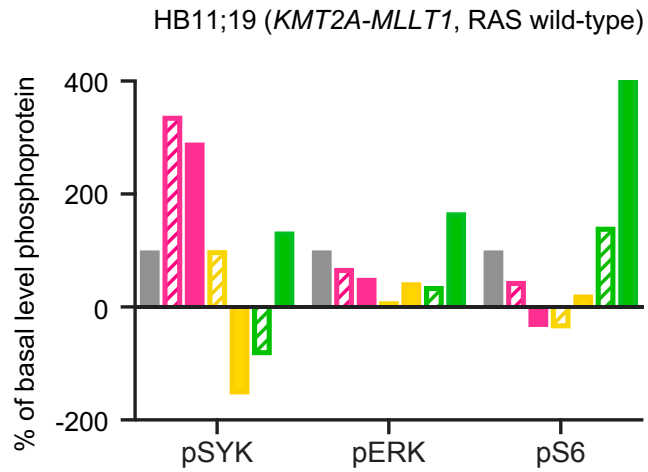
**A**



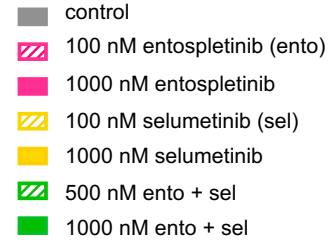
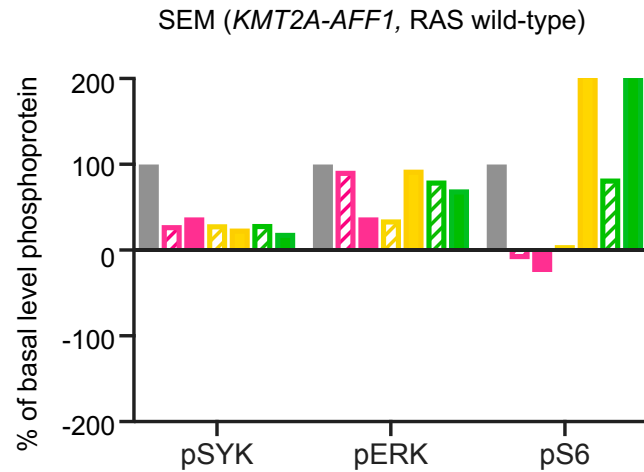
**B**



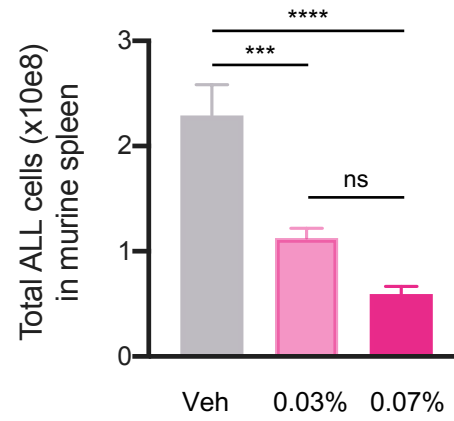
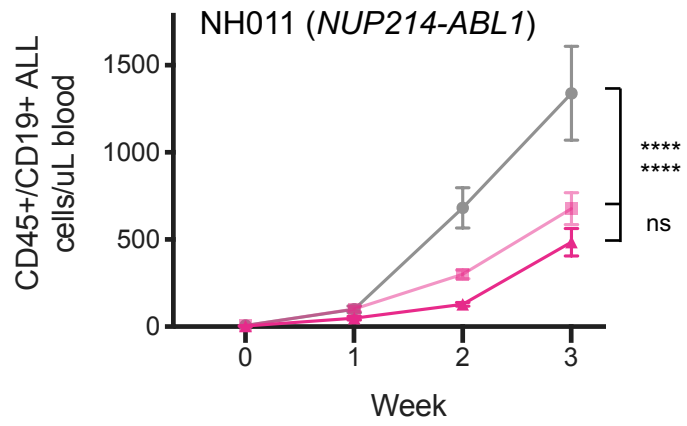
**C**



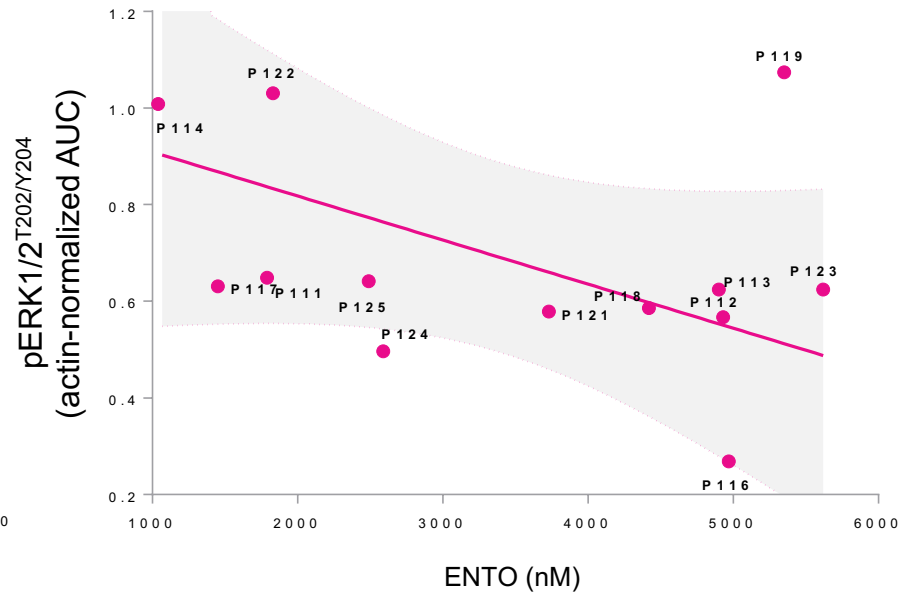
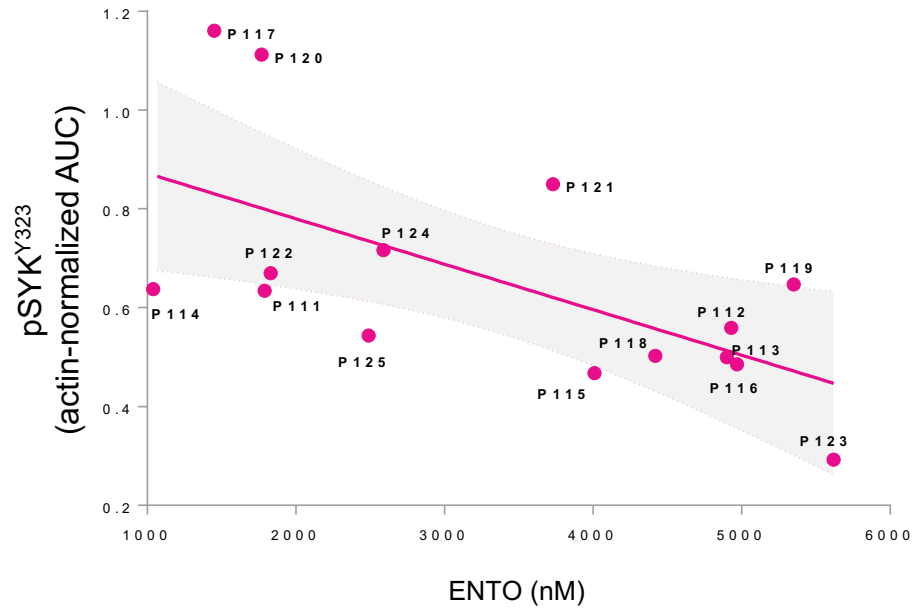
**D**



# Supplemental Figure 7

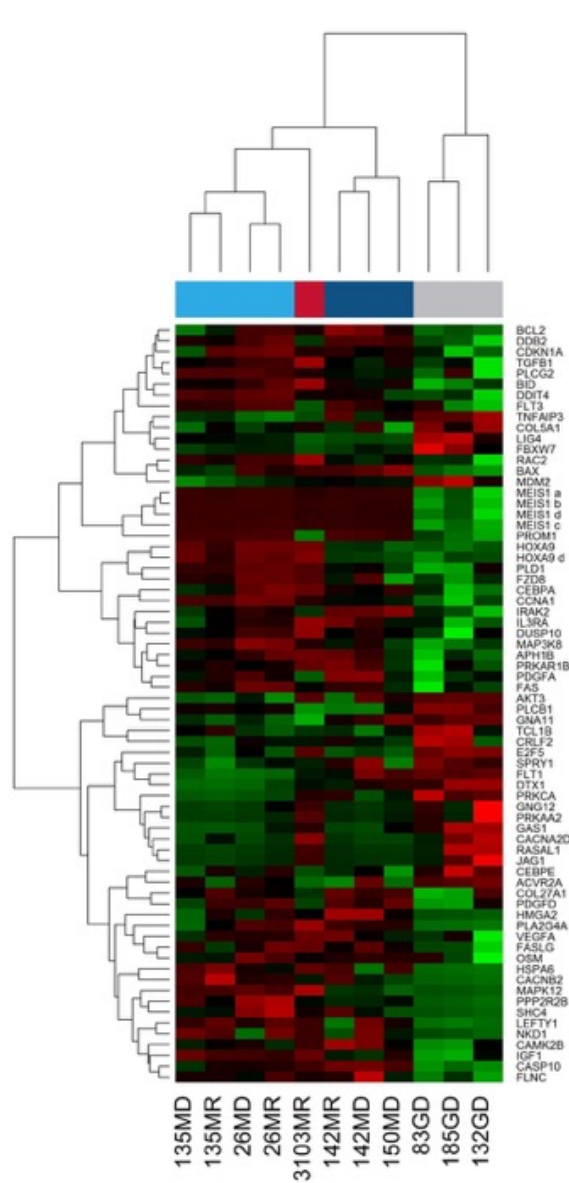


# Supplemental Figure 8

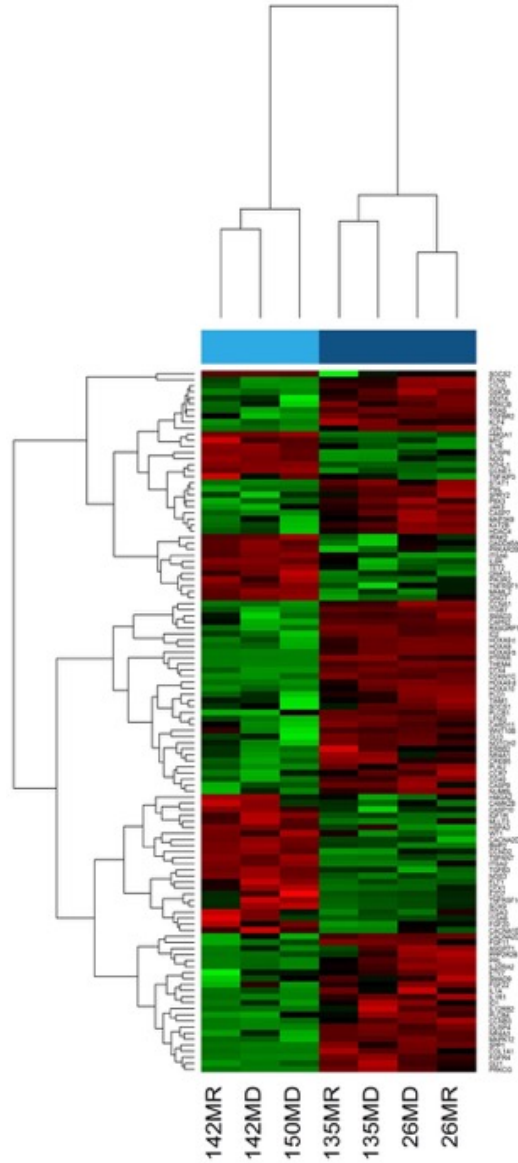


# Supplemental Figure 9

## A *KMT2A*-R vs non-*KMT2A*-R



## B *KMT2A*-AFF1 vs *KMT2A*-MLLT1



# Supplemental Figure 10

